J. Innovative Eng. Nat. Sci., vol. 4, no. 2, pp. 672-683, 2024.
http://doi.org/10.61112/jiens.1482541

Original Paper

Journal of Innovative Engineering and Natural Science
(Yenilikçi Mühendislik ve Doğa Bilimleri Dergisi)
https://dergipark.org.tr/en/pub/jiens

Nanocomposites obtained from various acrylate resins with DPGDA reactive diluent filled with fumed silica particles produced by using a DLP/LCD-type 3D printer

Mustafa Çakır[a], Emre Akın*[a]

[a]*Marmara University, Faculty of Technology, Metallurgical and Materials Engineering, İstanbul, Türkiye.*

ARTICLE INFO

Article history:
Received 11 May 2024
Received in revised form 10 June 2024
Accepted 22 July 2024

Available online

Keywords:
DLP/LCD-type 3D printer
DPGDA reactive diluent
Fumed silica nanoparticle
Acrylate resins

ABSTRACT

The present study presents various acrylate resin systems formulated with dipropylene glycol diacrylate (DPGDA) reactive diluent such as silicon acrylate (SiA), urethane acrylate (UA), and polyester acrylate (PEA) and their nanocomposites prepared by filling hydrophilic and amorphous fumed silica particles (FS) in different proportions produced by DLP (Digital Light Processing) and LCD (Liquid Crystal Display) (DLP/LCD) type 3D printers. The increase in the fumed silica content resulted in an increase in the ultimate tensile strength, the Young's modulus, the Izod impact strength, and the hardness values up to a certain value for each acrylate resin system. The PEA-DPGDA-2%FS nanocomposite showed an increase of 20.6% and 47.2% in the ultimate tensile strength and the Izod impact strength, respectively. A substantial increase in Izod impact strength of 61.7% was achieved with UA-DPGDA-1%FS. PEA-DPGDA and UA-DPGDA showed much higher mechanical properties than SiA-DPGDA. However, tensile strength, Young's modulus, and Izod impact strength of fumed silica-filled SiA-DPGDA samples showed substantial increases of 90%, 74.4%, and 60.8%, respectively.

I. INTRODUCTION

Over the past few years, there has been a surge of interest in the technology of 3D printing. From industrial manufacturing to personal use, this innovative technology has seen a remarkable expansion in its applications. The versatility of 3D printers has allowed them to be adopted in a wide range of sectors, facilitating advances in prototyping, customized medical implants, novel product designs in the food industry, and architectural endeavors [1, 2]. Reflecting its potential to revolutionize various industries, this growing enthusiasm for 3D printing has spurred continuous advancements and refinements in the field [3, 4]. In materials science and engineering, resins such as silicone acrylate, polyester acrylate, and urethane acrylate, which are commonly used for various industrial applications, are of great importance [5–7]. These resins are used in a wide range of applications and play a crucial role in advanced manufacturing techniques such as 3D printing [8]. Silicone acrylates are favored for their excellent elastic properties and chemical resistance [8, 9]. Polyester acrylates are known for their potential to provide high strength and durability [10, 11]. Urethane acrylates offer a wide range of uses because of their flexibility and combination of different mechanical properties [12, 13]. Reactive diluents combined with the main acrylate resins have a significant impact on mechanical, thermal, and physical qualities, in addition to the basic types of acrylate resins [14, 15]. When reviewing the literature, Kim and Seo [16] looked into how the mechanical properties of EB80 UV-cured commercial polyester acrylate resin were affected by a variety of reactive diluents, including hexanediol diacrylate (HDDA), tripropylene glycol diacrylate (TPGDA), and trimethylolpropane triacrylate (TMPTA). With HDDA, TPGDA, and TMPTA, they were able to reach

*Corresponding author. Tel.: +90-216-777-3931; e-mail: emre.akin@marmara.edu.tr

tensile strengths of 12.5 MPa, 14 MPa, and 18 MPa, respectively. Wang et al. [17] prepared different UV-cured polyester acrylate resins and compared them to a commercial polyester acrylate resin (Etercure 6387) that is a tri-functional oligomer. The synthesized different UV-cured polyester acrylate resins showed a tensile strength of 18.3 MPa and Shore D hardness of 47.9 when compared to the UV-cured Etercure 6387 resin. Additionally, adding filler to the resin system works well to achieve better qualities. Lahijania et al. [18] created UV-cured urethane acrylate nanocomposites by mixing non-treated and silane-treated nano-silica fillers with the resin while considering the literature. For the silane-treated silica-filled samples, they saw an increase in elastic modulus of 88%, compared to a 55% rise for the untreated silica-filled samples. For the silane-treated silica-filled samples, they saw a 200% increase in hardness, compared to a 91% rise for the untreated silica-filled samples. Sadej and Andrzejewska [19] employed a hybrid filler consisting of silica and aluminum oxide. They then compared the outcomes to those of fumed silica-reinforced polyethylene glycol diacrylate-based photocurable composites. The mechanical and thermal characteristics of both composites showed notable improvements. The samples containing fumed silica fillers showed an increase of 100% in Young modulus, but the samples containing silica/aluminum oxide hybrid fillers showed a 166% increase in Young modulus. Conversely, samples containing fumed silica fillers saw an increase in tensile strength of 81%, while samples containing silica/aluminum oxide hybrid fillers saw an increase in tensile strength of 45%. The samples with fumed silica fillers showed a 4% increase in Shore D hardness, whereas the samples with silica/aluminum oxide hybrid fillers showed a 5% increase in Shore D hardness. Prasertsri and Rattanasom [20] investigated the impact of fumed silica and participated silica fillers on the mechanical and thermal properties of natural rubber. When comparing the mechanical properties of fumed silica-reinforced natural rubber composites to those of silica fillers, they showed improved results. Preghenella et al. [21] prepared fumed silica-filled epoxy nanocomposites. The filled fumed silica particle ratios were varied from 0 to 9.2% by volume. While the fumed silica particles in the epoxy matrix for 3.3% and 6.4% increased the impact resistance and elongation, the ultimate tensile strength substantially decreased. The nanocomposite filled with the fumed silica particle of 9.2% showed a substantial increase in Young's modulus, while the fracture toughness was a little higher than that of the neat epoxy.

When evaluating the results related to the fumed silica-filled polymer-based composites in the literature, fumed silica has presented substantial improvements in terms of mechanical properties such as ultimate tensile strength, Young's modulus, and impact resistance. In this regard, this study aims to use fumed silica particles as filing material for various photopolymerizable resin systems for DLP/LCD-type 3D printers. Fumed silica was filled into the resin systems at concentrations ranging from 0 to 4%. It had a hydrophilic character and a particle size of about 20 nm. It is also a viable option for reinforcing polymer matrices due to its special qualities and range of uses. It has been shown that adding fumed silica particles to polymer resins increases their mechanical strength, thermal stability, and dimensional stability—all desirable properties [22–24]. Its branching and porous nature leads to a high surface area, and this high surface area provides high interfacial strength between the matrix and filler. As photopolymerizable main resins, commercial polyester acrylate, urethane acrylate, and silicon acrylate, which are widely used in industry for a variety of uses, were used in this investigation [25, 26]. Moreover, dipropylene glycol diacrylate (DPGDA) was used as a reactive diluent in these photopolymerizable resin systems. DPGDA is a difunctional reactive diluent and is generally used for applications that require improved flexibility, adhesion, and good moisture resistance [27, 28]. The mechanical properties of these products, such as their ultimate tensile strength, Young's modulus, tensile strain, notched-Izod impact resistance, and Shore D

hardness, were investigated. Moreover, the SEM morphologies of the fracture samples were observed following the tensile test.

II. EXPERIMENTAL METHOD

2.1 Materials

As main resins, commercial silicone diacrylate, urethane diacrylate, and polyester diacrylate were used. The product codes of these resins that were purchased from Allnex are EBECRYL® 350, EBECRYL® 284, and EBECRYL® 884. As a reactive diluent, dipropylene glycol diacrylate (DPGDA) that was acquired from BASF was used in each resin system. Fumed silica that was purchased from Wacker was used as filling material. Its product code is HDK N20 Aerosil 200 fumed silica. It is a pyrogenic, synthetic, hydrophilic, and amorphous silica nanoparticle and has a surface area of 200 m^2/g. The resin systems were cured using a Phrozen sonic mini resin DLP (Digital Light Processing) and LCD (Liquid Crystal Display) (DLP/LCD)-type 3D printer. Bis(2,4,6-trimethylbenzoyl)-phenylphosphine oxide (BAPO) was used as a photoinitiator. Its product code is IRGACURE® 819.

2.2 Preparation of fumed silica filled acrylate/DPGDA resins and curing by DLP/LCD type 3D printer

Three primary acrylate-based resin types were utilized: urethane diacrylate, silicon diacrylate, and polyester acrylate. DPGDA was used to dilute these resins. DPGDA increased the crosslinking density while reducing the viscosity of the primary resins. In addition, it was believed that the crosslinking reactions in the 3D printer would enhance the mechanical capabilities of the special flexible structure of DPGDA. Using DPGDA, each resin system was adjusted to 1/1 by weight. For ten minutes, these main resins and DPGDA were mechanically stirred in a beaker. Fumed silica particles were added to the resin systems in the concentration range of 0–4% after the homogenous mixture was obtained.

Table 1. The composition and code of the prepared samples

Sample	**Main resin**	**Reactive diluent**	**Ratio** (%wt.)	**Fumed silica** (%wt.)	**Photo initiator** (%wt.)
PEA-DPGDA	Polyester acrylate	DPGDA	50/50	-	5
PEA-DPGDA-1%FS	Polyester acrylate	DPGDA	50/50	1	5
PEA-DPGDA-2%FS	Polyester acrylate	DPGDA	50/50	2	5
PEA-DPGDA-3%FS	Polyester acrylate	DPGDA	50/50	3	5
PEA-DPGDA-4%FS	Polyester acrylate	DPGDA	50/50	4	5
UA-DPGDA	Urethane acrylate	DPGDA	50/50	-	5
UA-DPGDA-0.5%FS	Urethane acrylate	DPGDA	50/50	0.5	5
UA-DPGDA-1%FS	Urethane acrylate	DPGDA	50/50	1	5
UA-DPGDA-2%FS	Urethane acrylate	DPGDA	50/50	2	5
UA-DPGDA-3%FS	Urethane acrylate	DPGDA	50/50	3	5
UA-DPGDA-4%FS	Urethane acrylate	DPGDA	50/50	4	5
SiA-DPGDA	Silicon acrylate	DPGDA	50/50	-	5
SiA-DPGDA-1%FS	Silicon acrylate	DPGDA	50/50	1	5
SiA-DPGDA-2%FS	Silicon acrylate	DPGDA	50/50	2	5
SiA-DPGDA-3%FS	Silicon acrylate	DPGDA	50/50	3	5
SiA-DPGDA-4%FS	Silicon acrylate	DPGDA	50/50	4	5

Particularly for the 4% samples, it was found that the fumed silica particles raised the viscosity of the resin systems. The resin solutions were stirred simultaneously for one hour using both mechanical and ultrasonic means, following the addition of the fumed silica particles. A clean and uniform view of the filled resin systems was obtained after one hour of mechanical and ultrasonic stirring. To achieve a clear and uniform view, the filled resin systems were again stirred mechanically and ultrasonically for 45 minutes after adding BAPO photoinitiator at a weight concentration of 5%. The products were obtained during the curing process of the 3D printer after the transparent and homogenous resin systems were put into the resin tank. The composition and code of the prepared samples are given in Table 1.

2.3 Characterization of Test Specimens

For every weight percentage, three samples were prepared. The findings were calculated using the average of these three variables. The average results were used for each sample. Standard tensile tests were conducted in accordance with ASTM D638 TYPE 4 to determine Young's modulus, ultimate tensile strength, and elongation at maximum of the samples in order to define their mechanical properties. 5 mm/min was the crosshead speed used for the tensile testing. Using Zwick Z010 equipment, the tensile test was carried out at room temperature. IZOD impact test was carried out to measure the impact resistance of the notched samples in accordance with ASTM D 256. Zwick B5113.30 test apparatus with a 5.4J hammer and a 3.96 m/s striking rate was used. Shore D hardness test was also performed on the prepared samples to measure hardness values. After the tensile test, the fracture surface morphologies were examined using a Carl Zeiss Ultra Plus SEM (scanning electron microscope) at a voltage acceleration of 20 kV. Prior to the SEM investigations, the specimens were coated with 2-4 nm of Au/Pd using a Quorum Q150R device in an ion beam sputtering system.

III. RESULTS AND DISCUSSIONS

This research aims to systematically evaluate the mechanical properties of these novel composite materials, shedding light on the potential advantages and limitations associated with the introduction of fumed silica. The outcomes of this study not only contribute to the fundamental understanding of the synergies between fumed silica and acrylate-based resins but also provide valuable guidance for optimizing these composite materials for specific applications in industries such as coatings, adhesives, and advanced materials. In this context, the main resins mentioned were diluted with DPGDA reactive diluent. DPGDA is a difunctional reactive diluent and is generally used for applications that require improved flexibility, adhesion, and good moisture resistance [27, 28]. These acrylate-based resin systems were prepared by filling fumed silica particles in the 0-4% concentration range. Fumed silica had a hydrophilic character and a particle size of about 20 nm. It is also a viable option for reinforcing polymer matrices due to its special qualities and range of uses. It has been shown that adding fumed silica particles to polymer resins increases their mechanical strength, thermal stability, and dimensional stability—all desirable properties [29–31]. Its branching and porous nature leads to a high surface area, and this high surface area provides high interfacial strength between the matrix and filler. The surface area of the fumed silica particles employed in this study was 200 m^2/g. It was believed that the resin systems would increase the integrity of the particles, leading to an improvement in mechanical properties by impregnating the fumed silica

particles due to their branching and porous structure [32–34]. Tensile, Izod impact, and Shore D hardness tests were used to examine the mechanical properties of each system. Table 2 displays the tensile, impact, and hardness test results that were obtained.

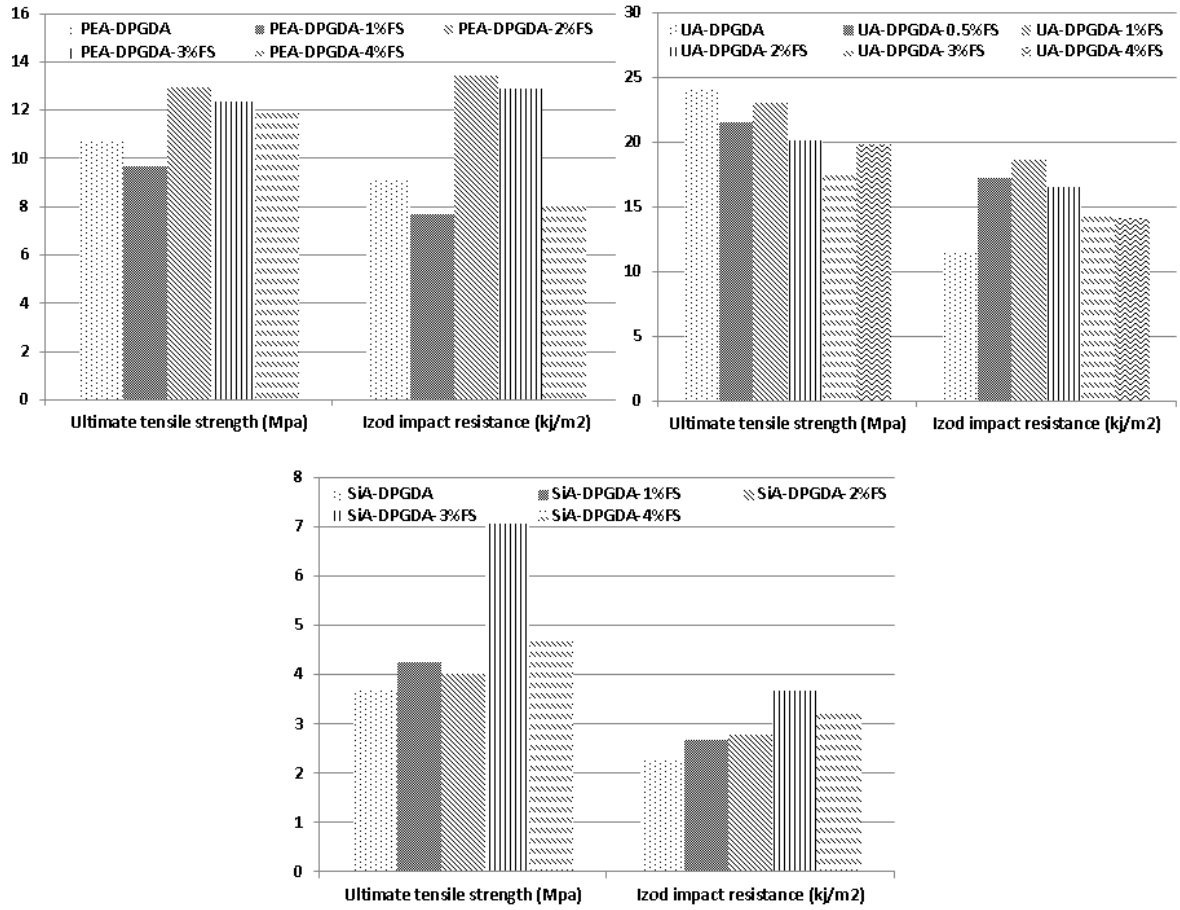

Figure 1. Comparative analysis of the trend of ultimate tensile strength and Izod impact resistance values for each sample

During the sample investigations, the ultimate tensile strength, Young's modulus, Izod impact resistance, and hardness values all increased with an increase in fumed silica concentration. Figure 1 and Figure 2 display the relative trend of these mechanical variables for every sample. For all resin systems, ultimate tensile strength and Izod impact resistance increased up to a specific filler ratio. The maximum values of ultimate tensile strength and Izod impact resistance for SiA-DPGDA and PEA-DPGDA samples were 3% and 2%, respectively, whereas that for UA-DPGDA samples was 1%.In addition, aside from ultimate tensile strength and Izod impact values, Young's modulus value increased for SiA/DPGDA while decreasing for UA-DPGDA and PEA-DPGDA samples due to the filled fumed silica particles. When evaluating all mechanical properties, the PEA-DPGDA-2%FS, UA-DPGDA-1%FS, and SiA-DPGDA-3%FS samples showed more enhanced properties. PEA-DPGDA-2%FS had an ultimate tensile strength value of 12.95 MPa, which represented an increase of 20.6%. In addition, Izod impact resistance increased by 47.2%. On the other hand, Young's modulus of PEA-DPGDA-2%FS indicated a slight decline of 8.6%. Young's modulus and ultimate tensile strength decreased for UA-DPGDA-1%FS. Young's modulus indicated a decrease of 21.8%, while tensile strength revealed a loss of 4%. While Young's modulus value remained within a rigid range, the decrease in the tensile strength modulus was negligible. In

addition to them, the Izod impact resistance value demonstrated a substantial increase of 61.7%. In comparison to SiA-DPGDA samples, PEA-DPGDA and UA-DPGDA samples showed much more enhanced mechanical properties. However, all mechanical parameters, including ultimate tensile strength, Young's modulus, and Izod impact resistance, were substantially increased when the fumed silica particle was added to the SiA-DPGDA resin system. There were increases of 90%, 74.4%, and 60.8% in the tensile strength, Young's modulus, and Izod impact resistance values, respectively. It might be explained by the fact that SiA-DPGDA samples had substantially lower mechanical characteristics than PEA-DPGDA and UA-DPGDA samples. Aside from these, the elongations of all nanocomposite samples were substantially increased by fumed silica particles. Therefore, the Izod impact resistance values substantially increased for all nanocomposite samples by adding fumed silica particles to the resin systems. According to Marouf et al. [35], plastics reinforced with microparticles can retard the propagation of cracks and increase fracture toughness. The fracture toughness of the polymer nanocomposite was enhanced by the size of the reinforcing silica particles, which ranged from 2 μm to 47 μm. The polymer nanocomposite was negatively affected by the silica particles between 200 and 1560 nm in size. In addition, for reinforcement particle sizes between 20 and 170 nm, there was minimal to no effect on fracture toughness. Similar results were found by Liang and Pearson [36] when they utilized silica particles in epoxy resin with particle sizes of 20 and 80 nm. When the volume proportion of particles is high, Marouf et al. [35] found out that achieving high fracture toughness values requires homogeneous filler dispersion. If not, agglomeration would cause the fracture toughness values to drop at high filler loading levels.

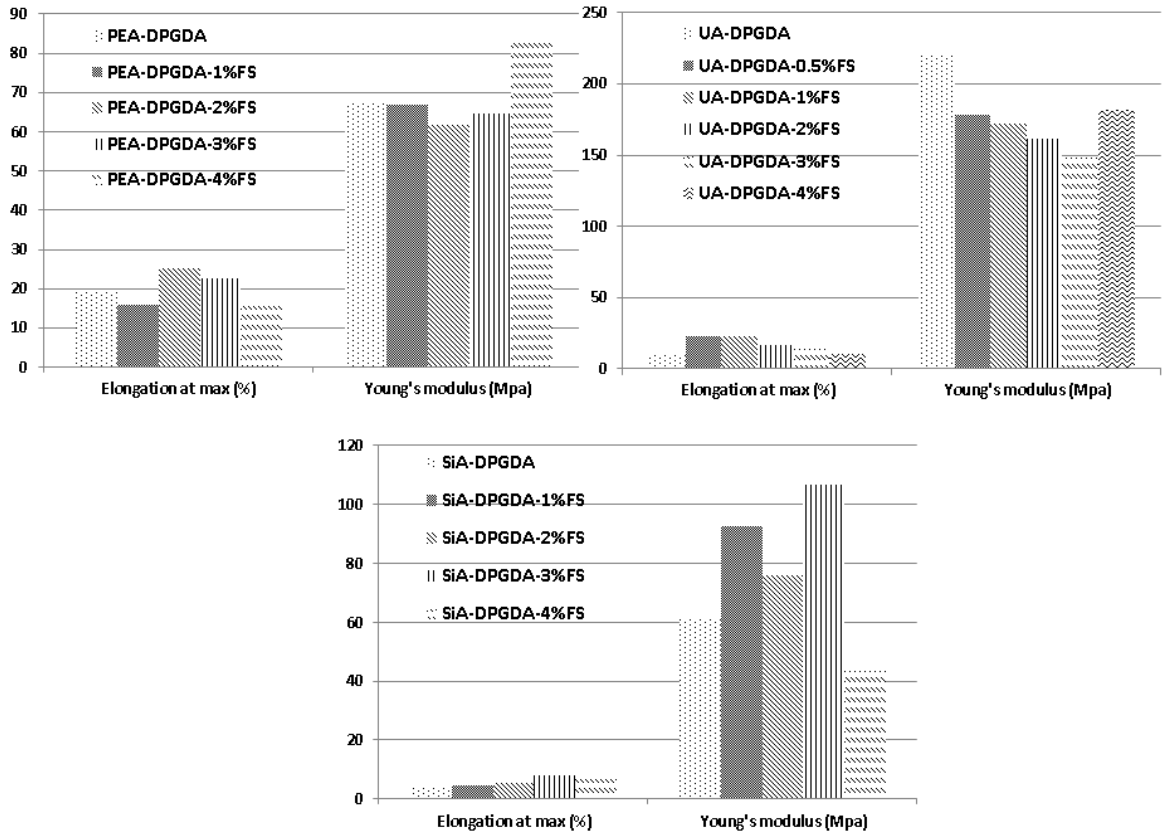

Figure 2. Comparative analysis of the trend of elongation at max and Young's modulus values for each sample

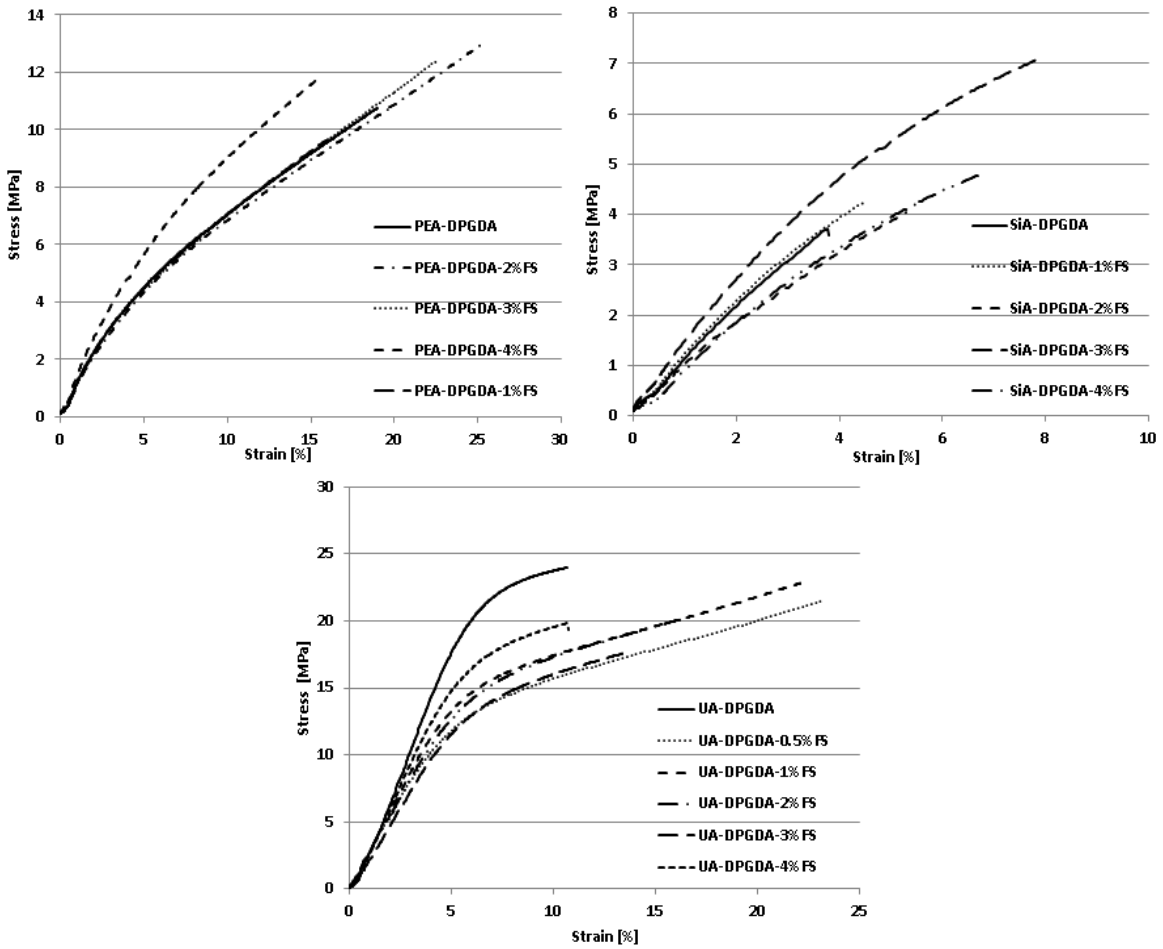

Figure 3. The average tensile stress-strain curves of the nanocomposites

Table 2. The mechanical values of the nanocomposites

Sample	Ultimate Tensile Strength (MPa)	Elongation at Break (%)	Young's Modulus (MPa)	Izod Impact (kJ/m^2)	Shore D Hardness
PEA-DPGDA	10.73	18.99	67.58	9.1	56
PEA-DPGDA-1%FS	9.66	16.02	66.92	7.7	55
PEA-DPGDA-2%FS	12.95	25.23	61.76	13.4	59
PEA-DPGDA-3%FS	12.37	22.52	64.63	12.9	57
PEA-DPGDA-4%FS	11.86	15.66	82.58	8.1	52
UA-DPGDA	23.96	10.67	220.33	11.5	63
UA-DPGDA-0.5%FS	21.48	23.13	178.73	17.2	66
UA-DPGDA-1%FS	22.98	22.43	172.25	18.6	67
UA-DPGDA-2%FS	20.12	16.28	161.7	16.5	62
UA-DPGDA-3%FS	17.72	13.74	148.76	14.5	61
UA-DPGDA-4%FS	19.82	10.66	181.62	14.1	59
SiA-DPGDA	3.72	3.77	61.26	2.3	34
SiA-DPGDA-1%FS	4.26	4.51	92.71	2.7	36
SiA-DPGDA-2%FS	4.04	5.29	75.96	2.8	37
SiA-DPGDA-3%FS	7.07	7.84	106.85	3.7	43
SiA-DPGDA-4%FS	4.76	6.67	43.41	3.3	37

When evaluating the Shore D hardness values of the samples, the results of Shore D hardness showed a similar trend with the other mechanical properties in terms of filled fumed silica ratio and used main resin. While UA-DPGDA samples showed the highest Shore D hardness values, the Shore D hardness values of PEA-DPGDA

samples were much higher than SiA-DPGDA samples. In terms of the prominent samples, Shore D hardness values presented the most enhanced values for the PEA-DPGDA-2%FS, UA-DPGDA-1%FS, and SiA-DPGDA-3%FS samples.

Table 3. The change ratios of the prominent samples compared to the neat samples in this study

Sample	**Ultimate Tensile Strength** (MPa)	**Young's Modulus** (MPa)	**Izod Impact** (kJ/m^2)
PEA-DPGDA	10.73	67.58	9.1
UA-DPGDA	23.96	220.33	11.5
SiA-DPGDA	3.72	61.26	2.3
		Changes in (±%)	
PEA-DPGDA-2%FS	+20.6	-8.6	+47.2
UA-DPGDA-1%FS	-4	-21.8	+61.7
SiA-DPGDA-3%FS	+90	+74.4	+60.8

Considering SEM morphologies in Figures 4 and 5, PEA-DPGDA, UA-DPGDA, and SiA-DPGDA were shown as neat samples, and PEA-DPGDA-2%FS, UA-DPGDA-1%FS, and SiA-DPGDA-3%FS were demonstrated as the prominent filled nanocomposite samples. It is well known that the overall smooth texture with river-line and textured microflow patterns represents the brittle fracture behavior. This situation was seen in PEA-DPGDA and SiA-DPGDA. The other neat sample, UA-DPGDA, showed more different fracture behavior that has many paths with wavy and cavity. These paths showed a certain amount of energy that was consumed for the tensile fracture. When evaluating the results of the neat samples, UA-DPGDA presented much more enhanced mechanical properties than PEA-DPGDA and SiA-DPGDA. SiA-DPGDA presented the poorest mechanical results. The SEM morphology of SiA-DPGDA showed the most distinct smooth texture with a river line and textured microflow pattern compared to the other neat samples. On the other hand, almost all the prominently filled nanocomposites in Figure 5 exhibited a homogeneous distribution. It is well known that homogeneous distribution is a key parameter for mechanical properties, especially impact resistance [35]. Additionally, particle size is a key parameter to obtain improved mechanical properties such as ultimate tensile strength, Young's modulus, and impact resistance values. While the particle sizes of PEA-DPGDA and SiA-DPGDA samples were mostly below 1 µm, UA-DPGDA presented mostly above the particle size of 1 µm. Moreover, the particle sizes around and above the particle size of 2µm were also available in the view of UA-DPGDA in Figure 5. [35, 21] As Marouf et al. [35] mentioned, silica particles with a homogeneous distribution around and above a particle size of 2 µm substantially affect fracture toughness. Besides the positive effect on ultimate tensile strength, a similar effect was observed above the particle size of 1 µm for UA-DPGDA samples. These effects differ for PEA-DPGDA and SiA-DPGDA samples because of their agglomerated particle sizes and the compatibility between matrix and fillers.

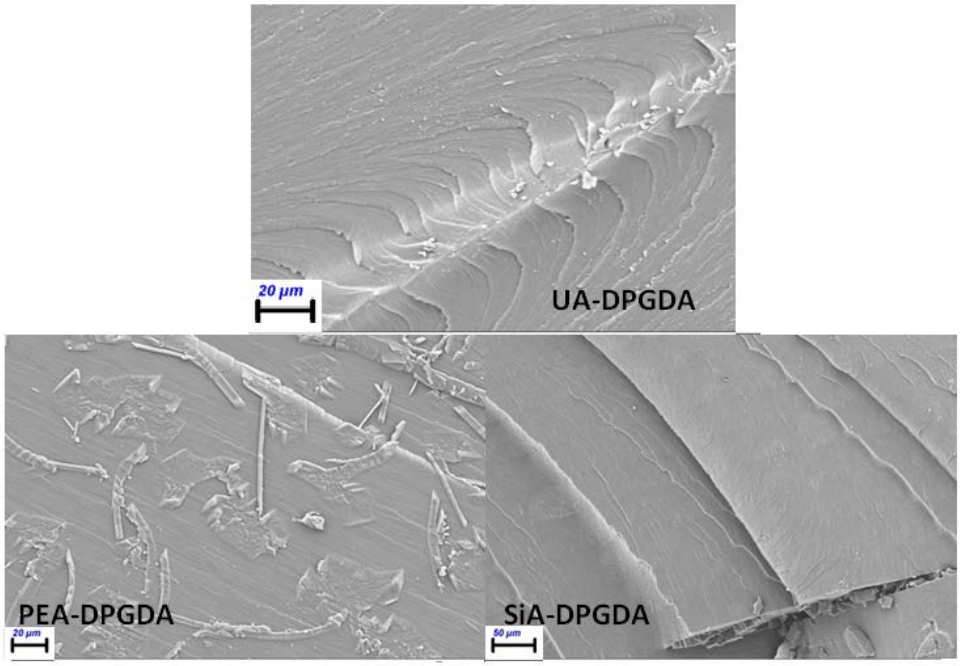

Figure 4. SEM morphologies of the neat samples

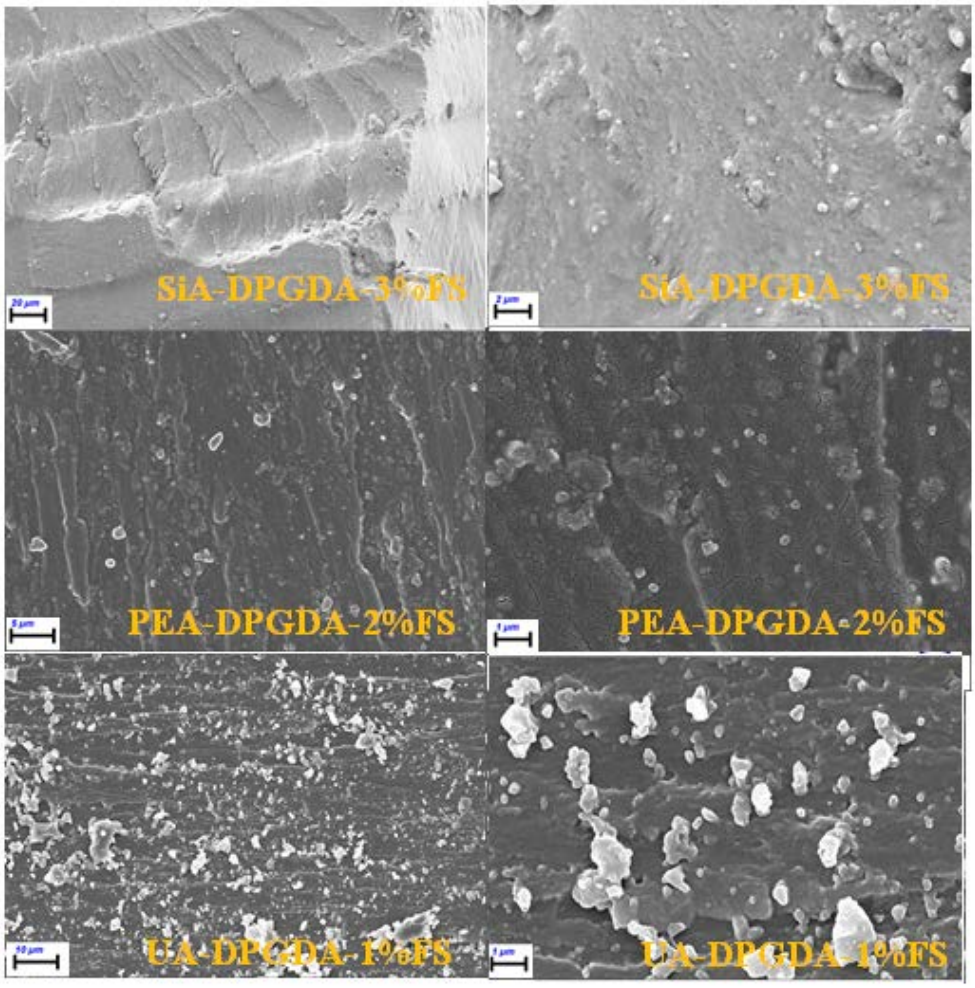

Figure 5. SEM morphologies of the prominent filled nanocomposite samples

Additionally, the maximal effect ratios varied for each sample. These ratios were 3%, 2%, and 1% for SiA-DPGDA, PEA-DPGDA, and UA-DPGDA samples. In contrast to the UA-DPGDA and PEA-DPGDA samples, the fumed silica particles in the SiA-DPGDA sample were less visible in the SEM morphology. The fumed silica particle and silicon matrix were believed to occur in a very high-integrity nanocomposite. The visibility of fumed silica particles for UA-DPGDA-1%FS is interestingly the highest among the other prominent nanocomposite samples, despite the higher ratios of PEA-DPGDA and SiA-DPGDA. As mentioned, fumed silica particles have a branching and porous structure. It was thought that PEA-DPGDA and SiA-DPGDA resins presented a more compatible structure to the fumed silica particles compared to UA-DPGDA in consequence of the impregnation of these resins into the branching and porous structure of the fumed silica particles. Therefore, more compatible visibility in SEM morphology was obtained between matrix and filling particles. When evaluating the results in Table 3, interesting trends in mechanical properties were observed by increasing the ratio of the samples. It is generally expected that reinforcing or filling materials increase some mechanical properties while the other one or more mechanical parameters decrease. For instance, when ultimate tensile strength or modulus values increase, Izod impact resistance decreases, or vice versa [25,37]. However, SiA-DPGDA-3%FS presented a different result. Substantial increases in ultimate tensile strength, Young’s modulus, and Izod impact resistance were observed for SiA-DPGDA-3%FS. PEA-DPGDA-3%FS presented substantial increases in ultimate tensile strength and Izod impact resistance, while a slight decrease in Young’s modulus was observed. Moreover, UA-DPGDA-1%FS presented substantial increases in Izod impact resistance and ultimate tensile strength while showing a negligible decrease in Young’s modulus. However, SEM morphologies showed that the fumed silica particles used in this study for UA-DPGDA samples had less compatibility with the matrix compared to the compatibility with the matrix of SiA-DPGDA and PEA-DPGDA samples. The fumed silica particles in the UA-DPGDA matrix presented a larger agglomeration compared to SiA-DPGDA and PEA-DPGDA. However, these particles in the matrix of UA-DPGDA dispersed homogeneously. They were also very efficient as the particles in the matrix of PEA-DPGDA and SiA-DPGDA. Especially, the improvement in Izod impact resistance was the highest compared to the other samples. Hence, it was observed that the fumed silica agglomeration above a particle size of 1μm is more efficient for the improvement of Izod impact resistance [38].

IV. CONCLUSIONS

The purpose of this study was to compare and enhance the mechanical properties of three distinct acrylate-based systems that contained DPGDA reactive diluent. Accordingly, different ratios of 1, 2, 3, and 4% of hydrophilic and amorphous fumed silica particles were added to these resin systems. These nanocomposites were manufactured using a DLP/LCD-type 3D printer. Tensile, Izod impact, and Shore D hardness tests were used to examine the mechanical properties of each reinforcing system. The study's findings indicate that the maximum tensile strength, Young's modulus, Izod impact resistance, and hardness values rose with the amount of fumed silica. For every resin system, the maximum tensile strength and Izod impact resistance increased up to a specific filler ratio. The maximum values of ultimate tensile strength and Izod impact resistance for SiA-DPGDA and PEA-DPGDA samples were 3% and 2%, respectively, whereas that for UA-DPGDA samples was 1%. In addition, aside from ultimate tensile strength and Izod impact values, Young's modulus value increased for SiA/DPGDA while decreasing for UA-DPGDA and PEA-DPGDA samples due to the filled fumed silica

particles. When evaluating all mechanical properties, the PEA-DPGDA-2%FS, UA-DPGDA-1%FS, and SiA-DPGDA-3%FS samples showed more enhanced properties. An increase of 20.6% was observed for the ultimate tensile strength value of PEA-DPGDA-2%FS. Additionally, an increase of 47.2% in Izod impact resistance was observed. On the other hand, Young's modulus of PEA-DPGDA-2%FS indicated a slight decline of 8.6%. Both the ultimate tensile strength and Young's modulus decreased for UA-DPGDA-1%FS. Young's modulus indicated a decrease of 21.8%, while tensile strength revealed a loss of 4%. Young's modulus was still at a level that might be regarded as rigid, and the decline in tensile strength modulus was negligible. A significant increase of 61.7% was observed in the Izod impact resistance. In comparison to SiA-DPGDA samples, PEA-DPGDA and UA-DPGDA samples showed much more enhanced mechanical properties. Nonetheless, every mechanical property, including ultimate tensile strength, Young's modulus, and Izod impact resistance, was substantially enhanced by the fumed silica particle loading into the SiA-DPGDA resin system. Increases of 90%, 74.4%, and 60.8% were observed in the tensile strength, Young's modulus, and Izod impact resistance, respectively.

REFERENCES

1. Cakir Yigit N, Karagoz, I (2023) A review of recent advances in bio-based polymer composite filaments for 3D printing. Polym Plast Technol Mater 62(9):1077-1095.
2. Karagöz İ, Bekdemir AD, Tuna Ö (2021) 3B yazıcı teknolojilerindeki kullanılan yöntemler ve gelişmeler üzerine bir derleme. Düzce Üniversitesi Bilim ve Teknoloji Dergisi 9(4):1186-1213.
3. Schittecatte L, Geertsen V, Bonamy D, Nguyen TT, Guénoun P (2023) From resin formulation and process parameters to the final mechanical properties of 3D printed acrylate materials. MRS Commun. https://link.springer.com/article/10.1557/s43579-023-00352-3
4. Dawood A., Marti B, Sauret-Jackson V, Darwood A (2015) 3D printing in dentistry. Br Dent J. https://www.nature.com/articles/sj.bdj.2015.914
5. Gopinathan J, Noh I (2018) Recent trends in bioinks for 3D printing. Biomater Res 22.
6. Kim HK, Ju HT, Hong JW (2003) Characterization of UV-cured polyester acrylate films containing acrylate functional polydimethylsiloxane. Eur Polym J 39:2235–2241.
7. Liu J, Jiao X, Cheng F, Fan Y, Wu, Yang X (2020) Fabrication and performance of UV cured transparent silicone modified polyurethane–acrylate coatings with high hardness, good thermal stability and adhesion. Prog Org Coat 144:105673.
8. Bagheri A, Jin J (2019) Photopolymerization in 3D Printing. ACS Appl Polym Mater 1: 593–611.
9. Davidson RS, Ellis R, Tudor S, Wilkinson, SA (1992) The photopolymerization of acrylates and methacrylates containing silicon. Polym 33:3031–3036.
10. Kim HK, Ju HT, Hong JW (2003) Characterization of UV-cured polyester acrylate films containing acrylate functional polydimethylsiloxane. Eur Polym J 39:2235–2241.
11. Jafarzadeh S, Claesson PM, Sundell P-E, Tyrode E, Pan J (2016) Active corrosion protection by conductive composites of polyaniline in a UV-cured polyester acrylate coating. Prog Org Coat 90:154–162.
12. Chen H, Lee S-Y, Lin Y-M (2020) Synthesis and Formulation of PCL-Based Urethane Acrylates for DLP 3D Printers. Polym 12:1500.
13. Deng Y, Li J, He Z, Hong J, Bao J (2020) Urethane acrylate-based photosensitive resin for three-dimensional printing of stereolithographic elastomer. J Appl Polym Sci 137.
14. Porcarello M, Mendes-Felipe C, Lanceros-Mendez S, Sangermano M (2024) Design of acrylated epoxidized soybean oil biobased photo-curable formulations for 3D printing. Sustain Mater Technol, 40: e00927.
15. Keck S, Liske O, Seidler K, Steyrer B, Gorsche C, Knaus S, Baudis S (2023) Synthesis of a Liquid Lignin-Based Methacrylate Resin and Its Application in 3D Printing without Any Reactive Diluents. Biomacromolecules 24:1751–1762.
16. Kim DS, Seo WH (2004) Ultraviolet-curing behavior and mechanical properties of a polyester acrylate resin. J Appl Polym Sci 92:3921–3928.
17. Wang J, Li J, Wang X, Cheng Q, Weng Y, Ren J (2020) Synthesis and properties of UV-curable polyester acrylate resins from biodegradable poly(l-lactide) and poly(ε-caprolactone). React Funct Polym 155:104695.

18. ZK Lahijania Y, Mohseni M, Bastani S (2014) Characterization of mechanical behavior of UV cured urethane acrylate nanocomposite films loaded with silane treated nanosilica by the aid of nanoindentation and nanoscratch experiments. Tribol Int, 69:10–18.
19. Sadej M, Andrzejewska, E (2016) Silica/aluminum oxide hybrid as a filler for photocurable composites. Prog Org Coat 94:1–8.
20. Prasertsri S, Rattanasom N (2012) Fumed and precipitated silica reinforced natural rubber composites prepared from latex system: Mechanical and dynamic properties. Polym Test 31:593–605.
21. Preghenella M, Pegoretti A, Migliaresi, C (2005) Thermo-mechanical characterization of fumed silica-epoxy nanocomposites. Polym 46:12065–12072.
22. Barthel H, Rösch L, J Weis (2005) Fumed Silica - Production, Properties, and Applications. In: N Auner, J Weis (eds) Organosilicon Chemistry II: From Molecules to Materials, Wiley, USA.
23. Dorigato A, D'Amato M, Pegoretti, A (2012) Thermo-mechanical properties of high density polyethylene – fumed silica nanocomposites: effect of filler surface area and treatment. J Polym Res 19.
24. Yue Y, Zhang H, Zhang Z, Chen Y (2013) Polymer–filler interaction of fumed silica filled polydimethylsiloxane investigated by bound rubber. Compos Sci Technol 86:1–8.
25. Aalto-Korte K (2012) Acrylic resins. In: SM John, JD Johansen, T Rustemeyer, P Elsner, HI Maibach (eds) Kanerva's Occupational Dermatology, 3rd edn. Springer, New York, pp 737–756.
26. Janani R, Majumder D, Scrimshire A, Stone A, Wakelin E, Jones AH, Wheeler NV, Brooks W, Bingham PA (2023) From acrylates to silicones: A review of common optical fibre coatings used for normal to harsh environments. Prog Org Coat 180:107557.
27. Jagtap AR, More A (2021) Developments in reactive diluents: a review. Polym Bull 79:5667–5708.
28. Wu G, Zang H, Zhang H (2020) Preparation and performance of UV-curable waterborne polyurethane prepared using dipentaerythritol hexaacrylate/dipropylene glycol diacrylate monomers. J Macromol Sci Part A 57:927–934.
29. Dalgakıran D, Deniz S (2023) Preparation and gas permeability properties of polyetherimide based nanocomposite membranes with fumed silica nanoparticles. Journal of Innovative Engineering and Natural Science 3(1):39–52.
30. MA Bahattab, V García-Pacios, J Donate-Robles, JM Martín-Martínez (2012) Comparative Properties of Hydrophilic and Hydrophobic Fumed Silica Filled Two-Component Polyurethane Adhesives. J Adhes Sci Technol 26:303–315.
31. Zhao J, Wu D, Han JY, Jin Z (2014) Mechanical Properties of Fumed Silica / HDPE Composites. AMM 633–634:427–430.
32. Liu CC, Maciel GE (1996) The Fumed Silica Surface: A Study by NMR. J Am Chem Soc 118:5103–5119.
33. Khavryutchenko AV, Khavryutchenko VD (2003) Fumed silica synthesis. Influence of hydrogen chloride on the fumed silica particle formation process. Macromol Symp, 194:253–268.
34. Hassanajili S, Sajedi MT (2016) Fumed silica/polyurethane nanocomposites: effect of silica concentration and its surface modification on rheology and mechanical properties. Iran Polym J, 25:697–710.
35. Marouf BT, Mai Y-W, Bagheri R, Pearson RA (2016) Toughening of epoxy nanocomposites: nano and hybrid effects. Polym Rev 56:70–112.
36. Liang YL, Pearson RA (2009) Toughening mechanisms in epoxy–silica nanocomposites (ESNs). Polym, 50:4895–4905.
37. PS S, Prasad V, Pahovnik D, Thomas S, Haponiuk JT, George SC (2022) Study the effect of fumed silica on the mechanical, thermal and tribological properties of silicone rubber nanocomposites. J Polym Res 29.
38. Arangure MI, Mora E, Macosko CW (1997) Compounding fumed silicas into polydimethylsiloxane: bound rubber and final aggregate size. J Colloid Interface Sci, 195: 329–337.